







## RESEARCH ARTICLE

Drivers of foliar  $^{15}\text{N}$  trends in southern China over the last century

Songbo Tang<sup>1,2,3,4</sup>  | Jianfeng Liu<sup>5</sup>  | Frank S. Gilliam<sup>6</sup>  | Peter Hietz<sup>7</sup>  |  
 Zhiheng Wang<sup>8</sup>  | Xiankai Lu<sup>1,2</sup>  | Feiyan Zeng<sup>1</sup> | Dazhi Wen<sup>1,2,3</sup> | Enqing Hou<sup>1,2</sup>  |  
 Yuan Lai<sup>1,2,3,4</sup> | Yunting Fang<sup>9</sup>  | Ying Tu<sup>9</sup> | Dan Xi<sup>9</sup> | Zhiqun Huang<sup>10</sup>  |  
 Dianxiang Zhang<sup>1</sup>  | Rong Wang<sup>11</sup>  | Yuanwen Kuang<sup>1,2,3</sup> 

<sup>1</sup>South China Botanical Garden, Chinese Academy of Sciences, Guangzhou, China

<sup>2</sup>Guangdong Provincial Key Laboratory of Applied Botany, South China Botanical Garden, Guangzhou, China

<sup>3</sup>Southern Marine Science and Engineering Guangdong Laboratory (Guangzhou), Guangzhou, China

<sup>4</sup>College of Resources and Environment, University of Chinese Academy of Sciences, Beijing, China

<sup>5</sup>Key Laboratory of Tree Breeding and Cultivation of National Forestry and Grassland Administration, Research Institute of Forestry, Chinese Academy of Forestry, Beijing, China

<sup>6</sup>Department of Biology, University of West Florida, Pensacola, Florida, USA

<sup>7</sup>Institute of Botany, University of Natural Resources and Life Sciences, Vienna, Austria

<sup>8</sup>Institute of Ecology and Key Laboratory for Earth Surface Processes of the Ministry of Education, College of Urban and Environmental Sciences, Peking University, Beijing, China

<sup>9</sup>Key Laboratory of Forest Ecology and Management, Institute of Applied Ecology, Chinese Academy of Sciences, Shenyang, China

<sup>10</sup>College of Geographical Sciences, Fujian Normal University, Fuzhou, China

<sup>11</sup>Shanghai Key Laboratory of Atmospheric Particle Pollution and Prevention (LAP3), Department of Environmental Science and Engineering, Fudan University, Shanghai, China

## Correspondence

Peter Hietz, Institute of Botany, University of Natural Resources and Life Sciences, Vienna 1180, Austria.

Email: [peter.hietz@boku.ac.at](mailto:peter.hietz@boku.ac.at)

Dianxiang Zhang, South China Botanical Garden, Chinese Academy of Sciences, Guangzhou 510650, China.

Email: [dx-zhang@scbg.ac.cn](mailto:dx-zhang@scbg.ac.cn)

Yuanwen Kuang, South China Botanical Garden, Chinese Academy of Sciences, Guangzhou 510650, China.

Email: [kuangyw@scbg.ac.cn](mailto:kuangyw@scbg.ac.cn)

## Funding information

National Natural Science Foundation of China, Grant/Award Number: 41771522; the Key Special Project for Introduced Talents Team of Southern Marine Science and Engineering Guangdong Laboratory, Grant/Award Number: GML2019ZD0408

## Abstract

Foliar stable nitrogen (N) isotopes ( $\delta^{15}\text{N}$ ) generally reflect N availability to plants and have been used to infer about changes thereof. However, previous studies of temporal trends in foliar  $\delta^{15}\text{N}$  have ignored the influence of confounding factors, leading to uncertainties on its indication to N availability. In this study, we measured foliar  $\delta^{15}\text{N}$  of 1811 herbarium specimens from 12 plant species collected in southern China forests from 1920 to 2010. We explored how changes in atmospheric  $\text{CO}_2$ , N deposition and global warming have affected foliar  $\delta^{15}\text{N}$  and N concentrations ([N]) and identified whether N availability decreased in southern China. Across all species, foliar  $\delta^{15}\text{N}$  significantly decreased by 0.82‰ over the study period. However, foliar [N] did not decrease significantly, implying N homeostasis in forest trees in the region. The spatiotemporal patterns of foliar  $\delta^{15}\text{N}$  were explained by mean annual temperature (MAT), atmospheric  $\text{CO}_2$  ( $\text{P}_{\text{CO}_2}$ ), atmospheric N deposition, and foliar [N]. The spatiotemporal trends of foliar [N] were explained by MAT, temperature seasonality,  $\text{P}_{\text{CO}_2}$ , and N deposition. N deposition within the rates from 5.3 to 12.6  $\text{kg N ha}^{-1} \text{ year}^{-1}$  substantially contributed to the temporal decline in foliar  $\delta^{15}\text{N}$ . The decline in foliar  $\delta^{15}\text{N}$  was not accompanied by changes in foliar [N] and therefore does not necessarily

Songbo Tang and Jianfeng Liu should be considered joint first author.

reflect a decline in N availability. This is important to understand changes in N availability, which is essential to validate and parameterize biogeochemical cycles of N.

#### KEYWORDS

atmospheric CO<sub>2</sub>, global change, foliar nitrogen concentrations, foliar nitrogen isotopes, nitrogen availability, nitrogen deposition

## 1 | INTRODUCTION

Global change has multiple ecological consequences on terrestrial ecosystems (Galloway et al., 2008). Nitrogen (N) availability, defined as the supply of N to terrestrial plants and soil microorganisms relative to their N demands (Schimel & Bennett, 2004), is essential in maintaining the structure and function of terrestrial ecosystems (Schmitz et al., 2019; Wolf et al., 2011). For instance, a decline of N availability will adversely affect plant growth and ecosystem productivity (Payne et al., 2017). While human activities have dramatically increased N input (Galloway et al., 2008; Payne et al., 2017), information on past N availability and thus on changes thereof is limited.

Nitrogen availability is frequently derived from the measurements of N concentrations ([N]) in soils, foliage and litter, and sometimes by direct N manipulation experiments or calculations of ecosystem N budgets (Wolf et al., 2011). In tropical and subtropical forests, the fast litter turnover, the high precipitation, and the large amount of N leaching limit the use of [N] in soils, foliage and litter to assess N availability (Krishna & Mohan, 2017). Using nutrient ratios of individual species as indicator of nutrient availability has also been questioned due to the substantial variations of nutrient (e.g., N) demand across taxonomic affiliation (Townsend et al., 2007). Assessments of N availability based solely on [N] or nutrient ratios of soils or plants may thus fail to account for N demand imposed by plant growth (Vitousek & Sanford, 1986).

Stable isotopes of N (expressed as  $\delta^{15}\text{N}$ ) in plant tissue typically increases with increasing N availability (Högberg, 1997). Ecosystems with high N availability are characterized by high rates of nitrification and denitrification, which tend to strongly discriminate against  $^{15}\text{N}$ , thus increasing soil and foliar  $\delta^{15}\text{N}$  (Elmore et al., 2016; Garten, 1993; Högberg, 1997), altering the uptake of  $^{14}\text{N}$  by nitrifying microbes. Under high N conditions, plants rely less on the mycorrhizae that fractionate N isotopes during N transfer to plants (Höbber & Högberg, 2012; Högberg, 1997). Previous estimates of changes in N availability inferred from tissue  $\delta^{15}\text{N}$  vary greatly with plant material used (foliage: Craine et al., 2018; McLauchlan et al., 2010; wood segments: McLauchlan et al., 2007 or tree rings: Hietz et al., 2011), contrasting ecosystems (grassland: Li et al., 2020 or forest: Hietz et al., 2010), and climatic regions (temperate: Gilliam et al., 2019, 2018; McLauchlan et al., 2017; or tropical: Hietz et al., 2010, 2011). These studies on changes in foliar  $\delta^{15}\text{N}$  and [N], however, were based on sometimes haphazard collections of samples wherein results might be affected by a systematic or geographic

bias over time, and generally did not considering additional factors that might affect a change in foliar  $\delta^{15}\text{N}$ .

Various factors of global change, including rising atmospheric CO<sub>2</sub> concentrations ([CO<sub>2</sub>]) (Luo et al., 2004), early spring caused by global warming (Elmore et al., 2016), increased atmospheric N deposition (Fang et al., 2011; Hietz et al., 2011; Hiltbrunner et al., 2019; Pardo et al., 2006; Vallano & Sparks, 2013), and changes in patterns of precipitation (Craine et al., 2009; Pardo et al., 2006; Tang et al., 2021), have been identified directly or indirectly to affect foliar  $\delta^{15}\text{N}$ . For example, seasonality of precipitation and temperature can negatively affect foliar  $\delta^{15}\text{N}$  by influencing plant productivity, N input, soil microbial activities, and litter decomposition (Asseng et al., 2011; Gremer et al., 2018; Tang et al., 2021). Low precipitation and high potential evapotranspiration (PET) could increase denitrification-driven N gas losses and decrease soil N leaching, thus increasing foliar  $\delta^{15}\text{N}$  (Gong et al., 2021; Houlton et al., 2006; Zhao et al., 2016). Increasing temperature might increase or decrease plant  $\delta^{15}\text{N}$  via stimulating N mineralization (increasing N supply, Craine et al., 2009; Pardo et al., 2006) or increasing plant growth (increasing N demand) due to prolonged growing season, respectively (Mason et al., 2022). In addition, increases in vapor pressure deficit (VPD) might increase plant  $\delta^{15}\text{N}$  via reduced N demand and absorption of plants due to decrease growth (Grossiord et al., 2020; Lihavainen et al., 2016; Yuan et al., 2019).

On global scales, decreases in foliar  $\delta^{15}\text{N}$  and [N] have been observed and interpreted as evidence of CO<sub>2</sub>-driven oligotrophication of terrestrial ecosystems (Craine et al., 2018). Changes in foliar  $\delta^{15}\text{N}$ , however, may also be caused by the direct and indirect effects of N deposition on plant  $\delta^{15}\text{N}$  (Hiltbrunner et al., 2019). Foliar  $\delta^{15}\text{N}$  can be affected by high N deposition if this results in a more open N cycle (Hietz et al., 2010, 2011). However, the isotopic composition of N deposition is affected by the sources of N (Hastings et al., 2009), and foliar  $\delta^{15}\text{N}$  can therefore be affected by the  $^{15}\text{N}$  signals of N deposition (Caldararu et al., 2022; Fang et al., 2011; Hastings et al., 2009; Hiltbrunner et al., 2019). Global increases of N deposition therefore create uncertainties and complications on the use of foliar  $\delta^{15}\text{N}$  as an indicator of N availability in ecosystems. Understanding changes in N availability is important to understand global change effects on ecosystems and to predict the effects of changing N deposition in ecosystems affected by the various drivers of global change.

Tropical and subtropical forests in southern China occupy a notably broad range in biotic and abiotic factors, including climate, biota, geological parent material, soils, and the history and frequency of disturbances (Zhou et al., 2014), and represent the

largest terrestrial sink for anthropogenic CO<sub>2</sub> emissions in China (Wang et al., 2020). Concurrently, the average rate of atmospheric N deposition over southern China has increased from 5 to 25 kg N ha<sup>-1</sup> year<sup>-1</sup> from the 1960s to the 2000s, although it has levelled off in the most recent years (Liu et al., 2011; Wang et al., 2017; Yu et al., 2019). Meanwhile, <sup>15</sup>N signals of N deposition have been altered due to the changes in the source of N deposition in southern China's cities, for example, Guiyang (Zhao et al., 2019). Data on long-term trends in foliar δ<sup>15</sup>N and [N] across a large area from southern China thus provide an opportunity to test the effects of various factors on foliar δ<sup>15</sup>N and [N] and to test how well changes in foliar δ<sup>15</sup>N reflect changes in N availability or might be explained by other factors. Here, we measured foliar δ<sup>15</sup>N and [N] of 1811 herbarium specimens and tested the following hypotheses: (1) Foliar δ<sup>15</sup>N and [N] decreased over the past 90 years (from 1920 to 2010) in southern China (18–34°N, 97–122°E, 1776 × 2775 km<sup>2</sup>), as seen in previous studies from temperate regions and at global scale, which has been interpreted as the effect of CO<sub>2</sub>-driven progressive N limitation (Craine et al., 2018; Luo et al., 2004); (2) alternatively, increase in N deposition resulted in increased foliar [N] but decreased foliar δ<sup>15</sup>N, due to the increased uptake of <sup>15</sup>N-depleted N from agricultural emissions (Fang et al., 2011; Qu et al., 2016); and (3) changes in temperature and precipitation are the main factors controlling the temporal variations of foliar δ<sup>15</sup>N in southern China, as the identified relationships between foliar δ<sup>15</sup>N and temperature and precipitation in other region or globally (Amundson et al., 2003; Craine et al., 2018). If foliar δ<sup>15</sup>N reflects N availability, we expect to see parallel changes in foliar [N] and their driving factors should be confirmed.

## 2 | MATERIALS AND METHODS

### 2.1 | Plant specimen collection and measurement

A total of 1811 herbarium specimens spanning 90 years (1920–2010) from 444 sites across subtropical and tropical forests of southern China (Figure S1, 18–34°N, 97–122°E) were obtained from the Herbarium of Southern China Botanical Garden, Chinese Academy of Sciences (<http://herbarium.scbg.cas.cn>). To minimize bias due to changing species composition or sample densities, we chose approximately equal numbers of samples from the same periods from five shrub and seven broad-leaved tree species belonging to nine families (Table S1), excluding legumes to avoid the effect of biological N fixation. The species are widely distributed in broad-leaved forests across subtropical and tropical China (Figure S1).

A small piece of leaf was carefully cut from each specimen, which had not been treated by any liquid for conservation and were not in contact with glue. Information on sampling location and date for each specimen was documented. All samples were dried at 65°C for 72 h and then finely milled for N isotope and concentration analysis by a mass spectrometer (MAT 253, Thermo Finnigan, North Pod Waltham, Massachusetts, USA) coupled with an elemental analyzer

(ECS4010, Costech Analytical Technologies, Valencia, California, USA).

### 2.2 | Data on abiotic factors

Gridded historic temperature and precipitation data with a resolution of one month and 1 km for southern China from 1920 to 2010 were extracted from Peng et al. (2019). Temperature seasonality (TS) from 1920 to 2010 was calculated from the gridded data as the standard deviation of monthly values

$$TS = SD\{Tav_{g_1}, Tav_{g_2}, \dots, Tav_{g_{12}}\}$$

where  $Tav_{g_1}, \dots, Tav_{g_{12}}$  indicate the mean temperature from January to December (Salazar & Mcnutt, 2012), and precipitation seasonality (PS) was calculated from the gridded data as

$$PS = \frac{SD\{PPT_1, \dots, PPT_{12}\}}{1 + \left(\sum_{i=1}^{12} PPT_i / 12\right)} \times 100$$

where  $PPT_1, \dots, PPT_{12}$  indicate the total precipitation from January to December (Fick & Hijmans, 2017; Salazar & Mcnutt, 2012).

Atmospheric [CO<sub>2</sub>] from 1920 to 2010 was obtained from NASA GISS (<https://data.giss.nasa.gov/modelforce/ghgases/>). Considering the correlation between altitude and atmospheric pressure, we used partial pressure of CO<sub>2</sub> ( $P_{CO_2}$ , Pa) rather than the CO<sub>2</sub> fraction for this study.  $P_{CO_2}$  was calculated as

$$P_{CO_2} = 10^{-6} \times CO_2 \times P_{atm}$$

where  $P_{atm}$  (Pa) is atmospheric pressure, which was calculated according to Allan et al. (1998)

$$P_{atm} = 101325 \times \left( \frac{298.15 - 0.0065 \times \text{Altitude}}{298.15} \right)^{5.26}$$

Potential evapotranspiration (PET) and vapor pressure (VAP) were extracted from Climate Research Unit (CRU) TS v3.26 with a spatial resolution of 0.5° × 0.5° (Harris et al., 2014). We calculated VPD from VAP and monthly temperature (Grossiord et al., 2020). Atmospheric N deposition (bulk deposition of NO<sub>x</sub> and NH<sub>y</sub>) in 1960, 1970, 1980, 1990, and the annual deposition rates between 1997 and 2010 were extracted from the grids with a spatial resolution of 1 × 1° modeled by Wang et al. (2017), who produced the long-term N deposition (1850–2100) using the global aerosol chemistry–climate model LMDZ-INCA, coupled with the LMDZ general circulation model and the INCA aerosol module. The models were based on the emission data including sea salt, oceanic emissions of NH<sub>3</sub>, vegetation emissions of NO, agricultural activities, and fuel combustion of NO<sub>x</sub> and NH<sub>y</sub>. Since the dataset from Wang et al. (2017) did not cover every year from 1920 to 1996, we produced the N deposition of each year during 1920–1996 via interpolation linearly based on the grids of 1850, 1960, 1970, 1980, 1990, and 1997.

## 2.3 | Statistical analyses

We tested the temporal patterns of foliar  $\delta^{15}\text{N}$ , [N] and environmental factors in southern China over the past 90 years via linear regressions for all species combined and for each species separately.

We used generalized additive mixed models (GAMM) to examine the relationship between foliar  $\delta^{15}\text{N}$  and [N] and environmental factors with the priori formulas: Foliar  $\delta^{15}\text{N} \sim 1 + s(\text{P}_{\text{CO}_2}) + s(\text{N deposition}) + s(\text{MAT}) + s(\text{MAP}) + s(\text{TS}) + s(\text{PS}) + s(\text{VPD}) + s(\text{PET}) + s(\text{Foliar [N]}) + (\text{site/species}) + \text{corCAR1}(\text{year}|\text{site/species})$  and Foliar [N]  $\sim 1 + s(\text{P}_{\text{CO}_2}) + s(\text{N deposition}) + s(\text{MAT}) + s(\text{MAP}) + s(\text{TS}) + s(\text{PS}) + s(\text{VPD}) + s(\text{PET}) + (\text{site/species}) + \text{corCAR1}(\text{year}|\text{site/species})$ . In the two formulas, site/species represents the random effect of species nested within sample site, and corCAR1 is an autocorrelation structure, which allows for unequally spaced observations; “s” indicates the corresponding covariate with smooth term (Marchand et al., 2020). After running the a priori models, we optimized the models via modifying the formulas based on estimated degree of freedom (EDF, Table S2). Specifically, factors with  $\text{EDF} \approx 1$  were set as linear terms, represented by “l” in the formulas (Marchand et al., 2020). Then, we ran the two new models to determine the relationships between foliar  $\delta^{15}\text{N}$  and [N] and factors. GAMMs were performed by the gamm function in the R package mcgv (Bartoń, 2018). We used the concurvity function in the R package mcgv to test the concurvity (a nonparametric analog of multicollinearity) between factors. The “Estimate” concurvity index of each factor lower than 0.5 indicates that the concurvity between factors is low (Zhao et al., 2022). Considering there might be inverse effects of an environmental factor at different levels on foliar  $\delta^{15}\text{N}$  or [N], we

assessed whether there were breakpoints in the smooth item in GAMMs visually, and determined the breakpoints via comparing fitting values.

We performed dominance analysis to calculate the incremental  $R^2$  ( $IR^2$ ) of each variable to foliar  $\delta^{15}\text{N}$  and foliar [N] (Azen & Budescu, 2003; Zhao et al., 2022). Single factors in the full GAMM were picked and fitted into the GAMM to develop a series of sub-models (Zhao et al., 2022). The  $IR^2$  of each environmental factor was derived via averaging all the difference between each possible sub-model excluding or including the relevant factor. The relative contribution of each factor was the percentage of the factor in total  $IR^2$  of all factors.

All analyses were performed in R software (version 4.1.0, R Core Team, 2020). Significance was set at  $p < .05$ .

## 3 | RESULTS

### 3.1 | Spatiotemporal patterns of foliar $\delta^{15}\text{N}$ and [N]

Foliar  $\delta^{15}\text{N}$  and [N] did not change in parallel with notable spatial variation in southern China over the past 90 years (Figures 1 and 2). For temporal trends, foliar  $\delta^{15}\text{N}$  significantly decreased by 0.82‰, from  $0.63 \pm 2.83\%$  in the 1920s to  $-0.19 \pm 2.86\%$  in the 2000s, whereas foliar [N] did not significantly change over the past 90 years (Figure 1). For spatial trends, foliar  $\delta^{15}\text{N}$  decreased from south to north (Figure 2a), but foliar [N] decreased from west to east, especially at lower latitude (Figure 2b). At the species level, foliar  $\delta^{15}\text{N}$  decreased (both significant and non-significant) across all the studied species whereas foliar [N] decreased in seven species and increased in the other five species (Figures S2 and S3).

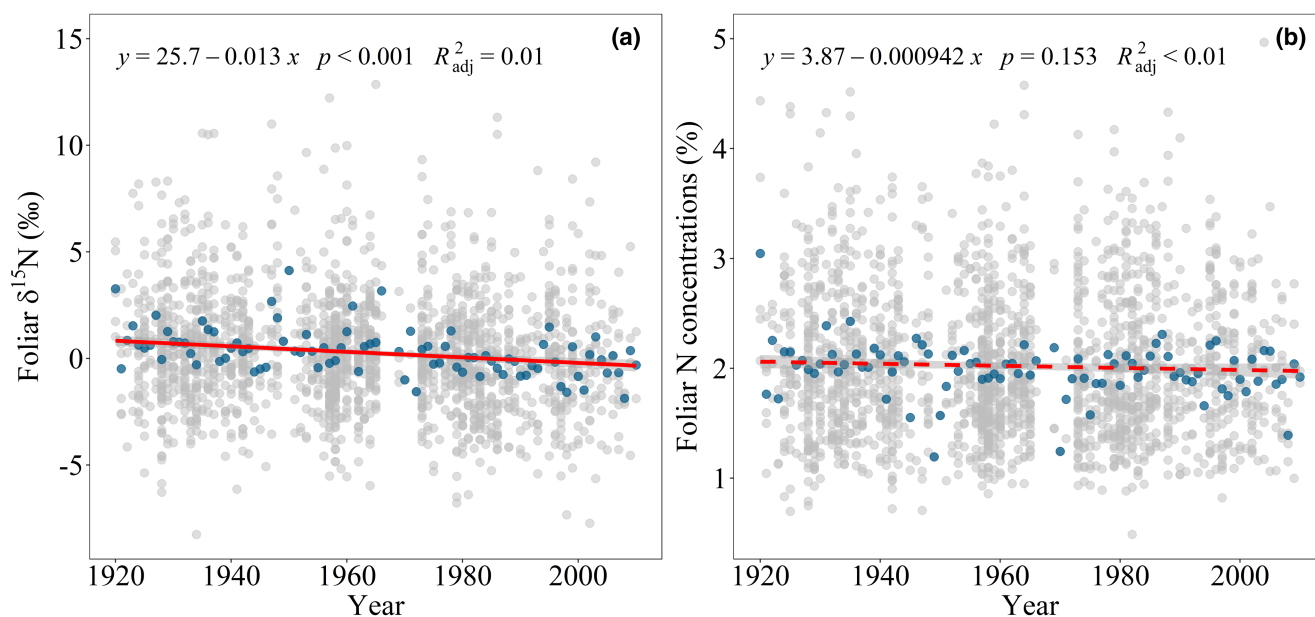


**FIGURE 1** Temporal patterns of foliar  $\delta^{15}\text{N}$  (a) and foliar [N] (b) of 12 species from southern China. Solid line indicates significant, and dashed red line indicates non-significant linear regression, at  $p < .05$  level. Fill areas indicate 95% interval confidence. Gray symbols represent individual samples ( $n = 1811$ ) and blue symbols annual mean values. [Colour figure can be viewed at [wileyonlinelibrary.com](http://wileyonlinelibrary.com)]

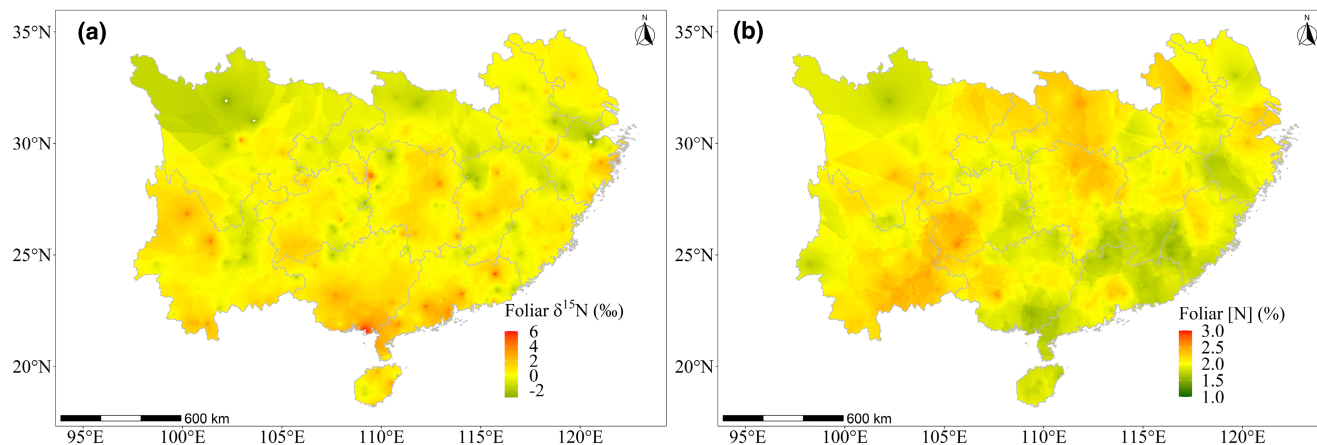


**FIGURE 2** Spatial patterns of foliar  $\delta^{15}\text{N}$  (a) and [N] [N concentrations, (b)] in south China. Figures are produced by Kriging interpolation using krige function in the gstat R packages. [Colour figure can be viewed at [wileyonlinelibrary.com](https://onlinelibrary.wiley.com/doi/10.1111/gcb.16285)]

**TABLE 1** Summaries of generalized additive mixed models (GAMMs)

| Variable                     | Factor                          | Unit                                     | EDF  | DF   | F      | RC (%) | p     | R <sup>2</sup> |
|------------------------------|---------------------------------|--|------|------|--------|--------|-------|----------------|
| Foliar $\delta^{15}\text{N}$ | P <sub>CO<sub>2</sub></sub> (s) | Pa                                       | 2.64 | 2.64 | 4.40   | 6.68   | .019  | .166           |
|                              | MAT (l)                         | °C                                       | 1.00 | 1.00 | 10.17  | 8.09   | .001  |                |
|                              | MAP (l)                         | mm                                       | 1.00 | 1.00 | 0.38   | 1.19   | .535  |                |
|                              | TS (s)                          | Unitless                                 | 2.55 | 2.55 | 0.86   | 4.72   | .297  |                |
|                              | PS (l)                          | Unitless                                 | 1.00 | 1.00 | 0.75   | <0.01  | .388  |                |
|                              | VPD (l)                         | kPa                                      | 1.00 | 1.00 | 3.14   | 0.66   | .076  |                |
|                              | PET (l)                         | mm                                       | 1.00 | 1.00 | 0.04   | 1.72   | .847  |                |
|                              | N deposition (s)                | kg N ha <sup>-1</sup> year <sup>-1</sup> | 4.04 | 4.04 | 3.09   | 8.31   | .016  |                |
|                              | Foliar [N] (s)                  | %  | 1.69 | 1.69 | 123.88 | 68.72  | <.001 |                |
| Foliar [N]                   | P <sub>CO<sub>2</sub></sub> (s) | Pa                                       | 2.57 | 2.57 | 6.40   | 29.38  | .002  | .023           |
|                              | MAT (s)                         | °C                                       | 3.14 | 3.14 | 2.91   | 16.48  | .031  |                |
|                              | MAP (l)                         | mm                                       | 1.00 | 1.00 | 0.03   | <0.01  | .853  |                |
|                              | TS (s)                          | Unitless                                 | 2.75 | 2.75 | 4.00   | 20.01  | .006  |                |
|                              | PS (l)                          | Unitless                                 | 1.00 | 1.00 | 0.61   | <0.01  | .434  |                |
|                              | VPD (s)                         | kPa                                      | 1.90 | 1.90 | 1.37   | 6.00   | .185  |                |
|                              | PET (s)                         | mm                                       | 2.65 | 2.65 | 2.90   | 6.67   | .096  |                |
|                              | N deposition (s)                | kg N ha <sup>-1</sup> year <sup>-1</sup> | 3.12 | 3.12 | 4.76   | 24.15  | .002  |                |

Note: "s" and "l" in parentheses after each variable indicated that smooth and linear term, respectively, was used in the equation of GAMMs.

Abbreviations: EDF, Estimated degree of freedom; Foliar [N], foliar nitrogen concentrations; MAP, mean annual precipitation; MAT, mean annual temperature; P<sub>CO<sub>2</sub></sub>, partial pressure of atmospheric CO<sub>2</sub> concentrations; PET, potential evapotranspiration; PS, precipitation seasonality; RC, relative contribution; TS, temperature seasonality; VPD, vapor pressure deficit.

### 3.2 | Drivers of spatiotemporal variation in foliar $\delta^{15}\text{N}$ and [N]

Between 1920 and 2010, the atmospheric [CO<sub>2</sub>] increased from 300 to 390 ppm, corresponding with mean P<sub>CO<sub>2</sub></sub> increased from 27 to 35 Pa, and N deposition in the study area increased with a strong spatial heterogeneity (Figures S4 and S5). Temperature seasonality decreased, while MAT, VPD, and PET increased with strong inter-annual variations (Figures S4, S6, and S7). P<sub>CO<sub>2</sub></sub>, N deposition,

and MAT were abiotic factors affecting the foliar  $\delta^{15}\text{N}$  and [N] over the past 90 years (Table 1; Table S2). Foliar  $\delta^{15}\text{N}$  correlated negatively with P<sub>CO<sub>2</sub></sub> (linearly) and intermedia rate of N deposition (about 5.3 kg N ha<sup>-1</sup> year<sup>-1</sup> to 12.6 kg N ha<sup>-1</sup> year<sup>-1</sup>), but positively with MAT (linearly), foliar [N] (nonlinearly), and low rate of N deposition (Figure 3 and Table 1). Foliar [N] correlated with P<sub>CO<sub>2</sub></sub> (negative, nonlinearly), MAT (positive, nonlinearly), TS (smoothly), and N deposition (nonlinearly) (Figure 4; Table 1). Assessing by the three-dimension plots, increases in N deposition would aggravate

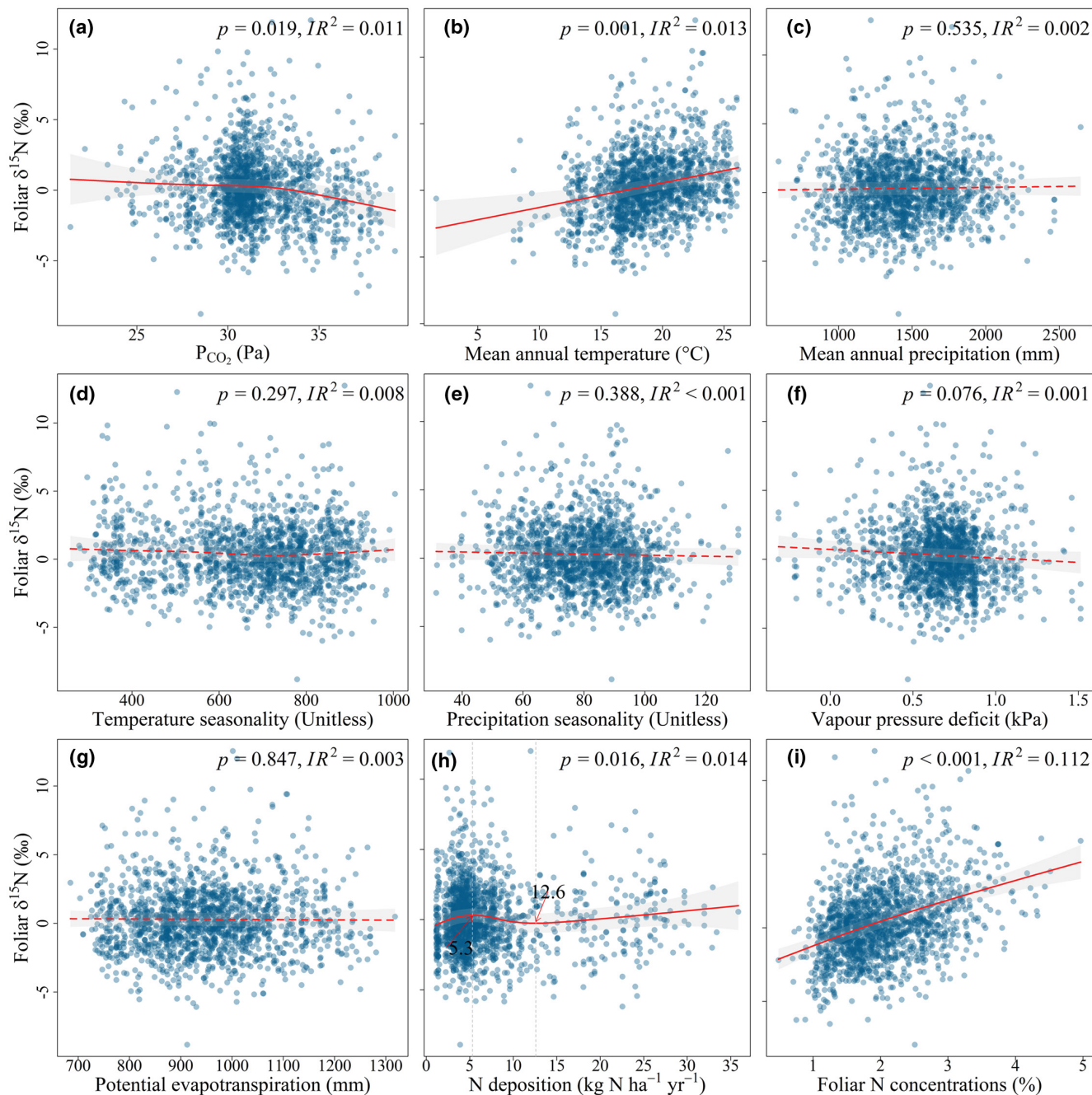


**FIGURE 3** Correlations between foliar  $\delta^{15}\text{N}$ , the environmental factors and foliar N concentrations derived from the generalized additive mixed models (GAMMs). Blue dots represent partial residuals from the generalized additive mixed models (GAMMs).  $IR^2$  indicates incremental  $R^2$  derived from dominance analysis. Red lines and gray shadings are, respectively, for the predicted values and 95% confidence intervals from the GAMMs. (a)  $P_{\text{CO}_2}$  (partial pressure of atmospheric  $\text{CO}_2$  concentrations), (b) Mean annual temperature, (c) Mean annual precipitation, (d) Temperature seasonality, (e) Precipitation seasonality, (f) Vapour pressure deficit, (g) Potential evapotranspiration, (h) N deposition, and (i) Foliar N concentrations. [Colour figure can be viewed at [wileyonlinelibrary.com](https://onlinelibrary.wiley.com)]

the negative effects of elevated  $P_{\text{CO}_2}$  on foliar  $\delta^{15}\text{N}$  when deposition rates were within  $5.3\text{--}12.6\text{ kg N ha}^{-1}\text{ year}^{-1}$ , and alleviate effects of elevated  $P_{\text{CO}_2}$  on foliar [N] when deposition rates were below  $18.9\text{ kg N ha}^{-1}\text{ year}^{-1}$  (Figures 3h, 4h, and 5). Correlations between foliar  $\delta^{15}\text{N}$  and each environmental factor were basically consistent among species (Figure S8), while correlations between foliar [N] and  $P_{\text{CO}_2}$ , MAT, N deposition, and TS were partly different among species (Figure S9a–c,h).

## 4 | DISCUSSION

We sampled 12 distributed rather homogeneously over space and time, providing an ideal dataset to search for the trends and drivers of long-term changes in foliar  $\delta^{15}\text{N}$  and [N]. Based on the dataset, we determined temporal and spatial patterns of foliar  $\delta^{15}\text{N}$  and [N] in southern China over the past 90 years. Consistent with part of our hypothesis 1, foliar  $\delta^{15}\text{N}$  decreased significantly; however, foliar [N]

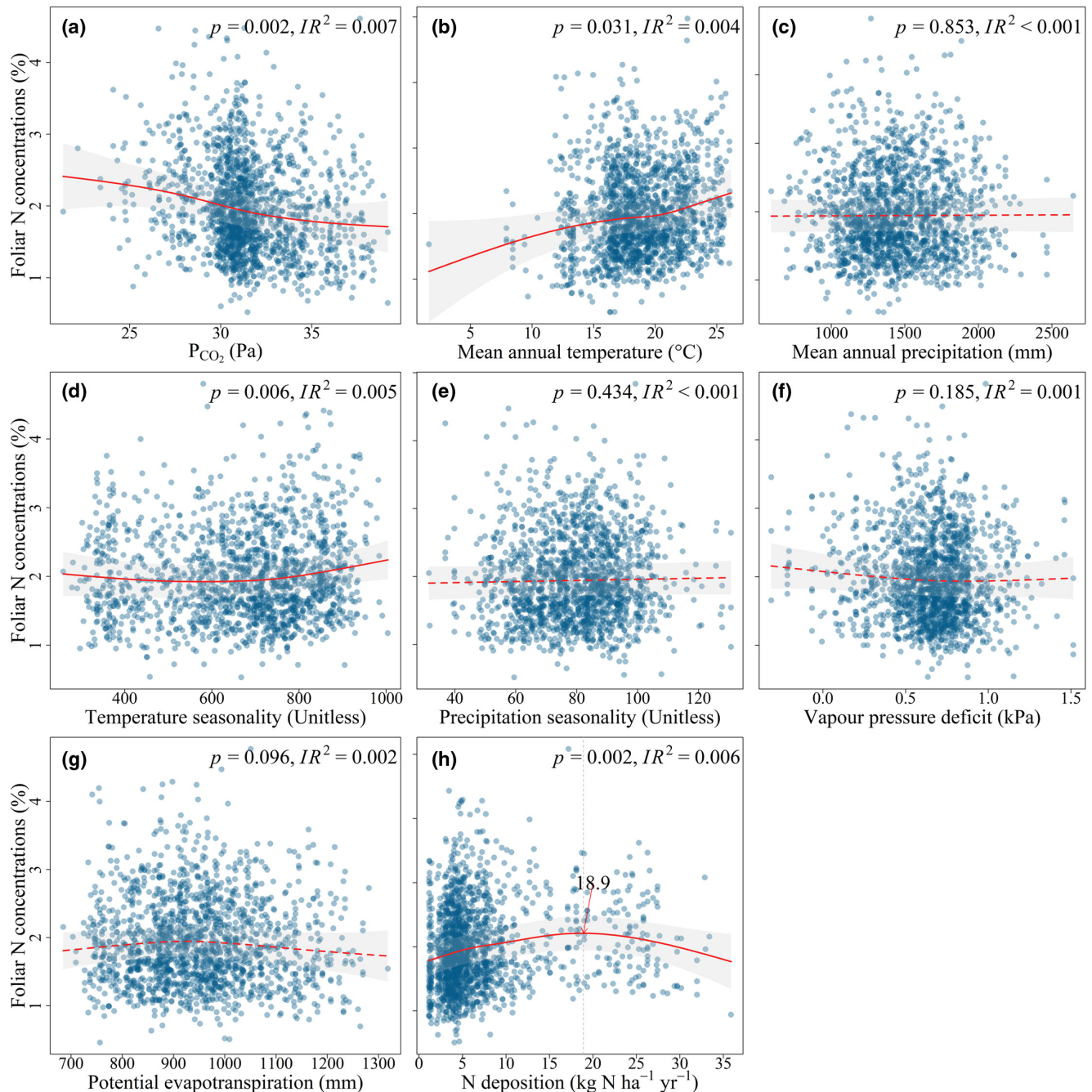


**FIGURE 4** Correlations between foliar N concentrations and the environmental factors derived from the generalized additive mixed models (GAMMs). Blue dots represent partial residuals from the generalized additive mixed models (GAMMs).  $IR^2$  indicates incremental  $R^2$  derived from dominance analysis. Red lines and blue shadings are, respectively, for the predicted values and 95% confidence intervals from the GAMMs. (a)  $P_{CO_2}$  partial pressure of atmospheric  $CO_2$  concentrations, (b) Mean annual temperature, (c) Mean annual precipitation, (d) Temperature seasonality, (e) Precipitation seasonality, (f) Vapour pressure deficit, (g) Potential evapotranspiration, and (h) N deposition. [Colour figure can be viewed at [wileyonlinelibrary.com](https://onlinelibrary.wiley.com/doi/10.1111/gcb.16385)]

did not significantly change. Spatiotemporal variations of foliar  $\delta^{15}N$  were related to changes in  $[CO_2]$  (-), N deposition (+/-), MAT (+), and foliar [N] (+), and the spatiotemporal variations of foliar [N] were associated with  $[CO_2]$  (-), N deposition (+/-), MAT (+), and TS (+), in partial support of our hypothesis 2. The complex effects of N deposition on foliar  $\delta^{15}N$  indicate that foliar  $\delta^{15}N$  does not necessarily reflect a decline in N availability. Significant effects of MAT, but not precipitation, on foliar  $\delta^{15}N$  highlights the consistency but also differences in

the response of N cycles to environmental factors between regional and global scales.

#### 4.1 | Trends in foliar $\delta^{15}N$ and [N]

In the present study, both the mean values (0.29‰ vs 0.4‰) and the range (-8.26‰ to 12.86‰ vs -20.6‰ to 21.4‰) of foliar  $\delta^{15}N$  are

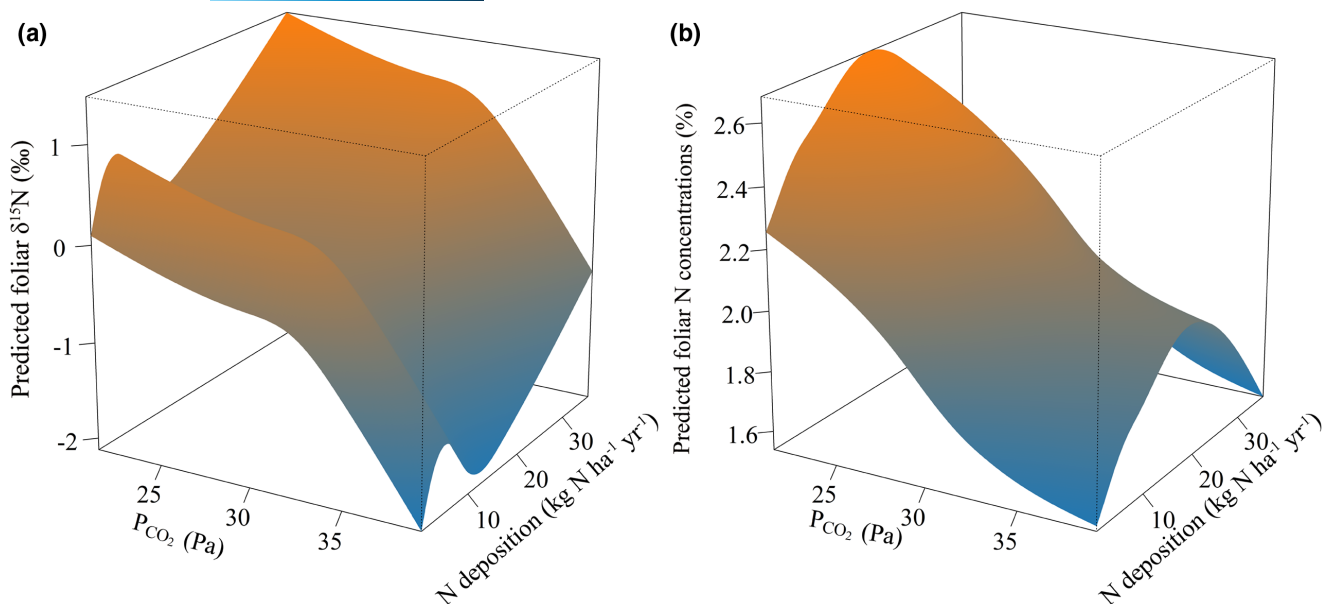


**FIGURE 5** The effects of N deposition and  $P_{CO_2}$  on foliar  $\delta^{15}N$  (a) and N concentrations (b) derived from the generalized additive mixed models (GAMMs) showed in three-dimensional interaction plots.  $P_{CO_2}$ , partial pressure of atmospheric  $CO_2$  concentrations. [Colour figure can be viewed at [wileyonlinelibrary.com](http://wileyonlinelibrary.com)]

smaller than those reported in a global dataset (Craine et al., 2018). Our data cover a substantial range in climate and N deposition, but were limited to a few well-replicated species, which strongly reduces the confounding effect of phylogeny, type of mycorrhiza, and nitrogen fixation on foliar  $\delta^{15}N$  and leaf [N] (Tables S1 and S3). The decrease in foliar  $\delta^{15}N$  from  $0.63 \pm 2.83\%$  in the 1920s to  $-0.19 \pm 2.86\%$  in the 2000s in this study is consistent with previous studies on leaves (McLauchlan et al., 2010; Peñuelas & Estiarte, 1997) or tree rings  $\delta^{15}N$  (McLauchlan et al., 2007) at either global or local scales, which has been interpreted as evidence for reduced N availability (Craine et al., 2018; McLauchlan et al., 2010) and explained by  $CO_2$ -driven progressive N limitation (Luo et al., 2004, 2006). Increasing N limitation, however, appears implausible in regions such as southern China, with a strong increase in anthropogenic N emissions and consequent N deposition (Liu et al., 2011; Yu et al., 2019). By contrast, foliar or woody tissue  $\delta^{15}N$  increased in several tropical forests (Hietz et al., 2010, 2011), which was interpreted as the effect of N deposition and more open N cycles, or did not change (van der Sleen et al., 2015) during the 20th century.

The interpretation of  $\delta^{15}N$  as an indicator of N availability was supported by parallel decrease (Craine et al., 2018) or increases (Hietz et al., 2011) of foliar [N]. In our study, the temporal trends of declining foliar  $\delta^{15}N$  were not accompanied by statistically significant declines in foliar [N] (Figure 1). While we found a relatively strong positive correlation between foliar  $\delta^{15}N$  and [N] consistent with prior observations (Figure 3i), long-term changes in foliar  $\delta^{15}N$  are apparently decoupled from changes in foliar [N]. This might be because increasing N deposition, which increases N availability, and  $[CO_2]$ , which reduce foliar [N] cancel each other out, or else changes in foliar  $\delta^{15}N$  are not affected by N availability alone, as suggested by the negative correlation between foliar [N] and  $P_{CO_2}$  and the positive correlations between foliar [N] and low-rate

N deposition. Here, it should be pointed out that the correlations between N deposition and foliar [N] became negative at N deposition rates above c.  $18.9 \text{ kg N ha}^{-1} \text{ year}^{-1}$ , which might result from the decreasing plant N uptake under high N deposition due to soil acidification and/or nutrient imbalance (Lu et al., 2014; Pan et al., 2020). In our dataset, there were rather few observations with high N deposition, so the effect of excessive N deposition on N availability, which will depend on soils and other factors, warrants further studies.

The constant foliar [N] observed over the past 90 years in the present study differs from the decrease observed at global scale during 1980–2010 (Craine et al., 2018), and the increases related to anthropogenic N deposition in Panama (Hietz et al., 2011) and whole China (Liu et al., 2013). The homeostasis of foliar [N] in forest trees in southern China is surprising given the strong increase in N deposition in the studied regions since 1960 (Figures S4h and S5). It is worth mentioning that the discrepancies between Liu et al. (2013) and the present study might be caused by unsystematic and unbalance sampling in the former study (Pardo et al., 2013). The 981 observations of plant foliar [N] in Liu et al. (2013) included 666 species from across China, while our 1811 specimens only included 12 species from southern China. The variable change in species composition over time and difference in species' response to various factors controlling foliar N could therefore explain differences among studies (Pardo et al., 2013). Additionally, although increased N deposition can potentially increase foliar [N], progressive N limitation by elevated atmospheric  $[CO_2]$  could have countered the effect of N deposition (Luo et al., 2004), which can be supported by the correlations between foliar [N] and N deposition,  $P_{CO_2}$ , and the temporal trends of foliar [N] before and after 1960 (Figure 3a,h; Figure S10b). Whatever the cause of the constant foliar [N] in our dataset, this pattern deserves explanation. Therefore, we systematically analyzed



the effects of various factors including  $[\text{CO}_2]$ , climate, and N deposition potentially affecting foliar  $\delta^{15}\text{N}$ .

## 4.2 | Multiple factors influencing foliar $\delta^{15}\text{N}$

Various environmental factors affect foliar  $\delta^{15}\text{N}$  via influencing plant N availability or otherwise (Craine et al., 2009; Evans, 2001; Högberg, 1997). The correlations between foliar  $\delta^{15}\text{N}$  and the environmental factors that we found (Figure 3) coincide well with the patterns reported across other regions of China (Tang et al., 2021) and globally (Craine et al., 2009). In addition to climate and soil (Fang et al., 2011), foliar  $\delta^{15}\text{N}$  was also negatively correlated with  $\text{P}_{\text{CO}_2}$  (Figure 4a). Increasing  $\text{P}_{\text{CO}_2}$  leads to enhanced photosynthesis and growth in plants (BassiriRad et al., 2003), which increases the demand and absorption of N and decreases N availability (Luo et al., 2004, 2006). The correlations between foliar  $\delta^{15}\text{N}$  and temperature were consistent with both Craine et al. (2018) and Amundson et al. (2003). Although increases in temperature may prolong the growing season (Elmore et al., 2016), increases in mean annual temperature might enhance the process of soil N mineralization and increase the losses of  $^{15}\text{N}$ -depleted N, resulting in high plant N availability and/or high foliar  $\delta^{15}\text{N}$  (Amundson et al., 2003; Dai et al., 2020; Pardo et al., 2006). In contrast to Craine et al. (2018) and Amundson et al. (2003), we did not observe the positive correlation between foliar  $\delta^{15}\text{N}$  and MAP, suggesting that forests can be affected by different factors in different regions.

Notably, both the correlations between N deposition and foliar  $\delta^{15}\text{N}$  and N deposition and foliar [N] were non-linear and affected by the N deposition rate (Figures 3h, 4h, and 5). These results might help to explain the sometimes-conflicting observations of relationships between N deposition and changes in plant  $\delta^{15}\text{N}$  (Hietz et al., 2011; McLaughlan et al., 2017; Peñuelas & Filella, 2001; Vallano & Sparks, 2013).

In general, we expected foliar  $\delta^{15}\text{N}$  to increase continually with the increasing N deposition due to increase in N availability, but the reverse also has been reported in various ecosystems (Fang et al., 2011; Felix et al., 2017; Li et al., 2020; Peñuelas & Filella, 2001; Vallano & Sparks, 2013). Changes in N deposition, however, can affect foliar  $\delta^{15}\text{N}$  either by changes in N cycle or by the direct  $\delta^{15}\text{N}$  signal of deposition. In the first case, we would expect to see an increase in ecosystem and foliar  $\delta^{15}\text{N}$  with deposition, which is opposite to what we found. In the second case, the effect will depend on the  $\delta^{15}\text{N}$  signal and the amount of N deposited. Although agricultural fertilizer has a  $\delta^{15}\text{N}$  signal close to 0, due to fractionation by gaseous losses, atmospheric  $\text{NH}_y$  derived from the fertilizer has negative signal (Liu et al., 2008; Qu et al., 2016). Therefore, increasing use of N fertilizers might explain the decline in foliar  $\delta^{15}\text{N}$ . When N input has reached a level of ecosystem saturation, N losses increase, resulting in increasing soil and foliar  $\delta^{15}\text{N}$ , which can explain the positive correlation between foliar  $\delta^{15}\text{N}$  and N deposition under high N deposition (Figure 3h). Besides, the main source of atmospheric N deposition changed from agricultural ( $\text{NH}_y$ ) to industry ( $\text{NO}_x$ , e.g.,

traffic emissions), which might also contribute to the rate-dependent relationship. Early on, sources of atmospheric N in Guiyang, one of regions in our study, were urban sewage and agricultural  $\text{NH}_y$ , which was characterized by low  $\delta^{15}\text{N}$  (Liu et al., 2008; Qu et al., 2016). During 2006–2017, the dominant atmospheric N compounds and sources changed from  $^{15}\text{N}$ -depleted  $\text{NH}_y$  (–15~0‰) to less depleted or  $^{15}\text{N}$ -enriched  $\text{NO}_x$  (–5~5‰, Felix & Elliott, 2014; Heaton, 1990; Liu et al., 2008; Rivero-Villar et al., 2018; Shan et al., 2019) in urban regions (Zhao et al., 2019), which might affect the  $\delta^{15}\text{N}$  in leaves. The change in the form of N in deposition was slow and occurred in the later period covered by our study (Yu et al., 2019; Zhao et al., 2019), allowing for decreases in foliar  $\delta^{15}\text{N}$  of trees in southern China over the past 90 years. Given the lower spatial resolution of N deposition data used in the present study, further studies based on long-term data of N deposition with higher spatial resolution should be conducted to refine the rate-dependent relationships between N deposition and foliar  $\delta^{15}\text{N}$ .

## 4.3 | Nitrogen deposition affects the use of foliar $\delta^{15}\text{N}$ as an indicator of N availability

Using a balanced design with samples from regions of strongly increasing and regionally variable N deposition, we found that MAT, N deposition,  $\text{P}_{\text{CO}_2}$ , and foliar [N] can affect foliar  $\delta^{15}\text{N}$ . These factors drive the changes in foliar  $\delta^{15}\text{N}$  in different directions where increasing MAT would increase, increasing  $\text{P}_{\text{CO}_2}$  would decrease foliar  $\delta^{15}\text{N}$ , and the effect of N deposition depends on the rate and signal of N deposition. Although we do not question the general relationship between ecosystem  $\delta^{15}\text{N}$  and N saturation, under conditions of changing N deposition plant  $\delta^{15}\text{N}$  signals are more challenging to interpret. Increased atmospheric deposition of N in southern China (Figures S4h and S5; Lu & Tian, 2014; Yu et al., 2019) should have increased N availability, foliar [N], and foliar  $\delta^{15}\text{N}$  as found in tropical forests (Hietz et al., 2011). However, the rate-dependent relationship between foliar  $\delta^{15}\text{N}$  and N deposition and the relative stable foliar [N] over the past 90 years found in the present study suggest that the decreasing trends of foliar  $\delta^{15}\text{N}$  may not always indicate a decrease in N availability. Therefore, the form of N, its isotopic composition, and rates of N deposition should be considered when assessing N availability based on foliar  $\delta^{15}\text{N}$ .

### AUTHOR CONTRIBUTIONS

K. Y. and Z. D. designed the study; T.S., X. D., and Z. F. performed the experiments; T. S., L. J., H. P., and K. Y. collected and analyzed the data; T. S., L. J., K. Y., H. P., and F.S.G. drafted the manuscript; all authors revised the manuscript.

### ACKNOWLEDGMENTS

This study was jointly supported by the National Natural Science Foundation of China (No. 41771522), the Key Special Project for Introduced Talents Team of Southern Marine Science and Engineering Guangdong Laboratory (No. GML2019ZD0408).

## CONFLICT OF INTEREST

The authors declare no conflict of interest.

## DATA AVAILABILITY STATEMENT

The data of the foliar  $\delta^{15}\text{N}$  and N concentrations of all samples and R codes used in this manuscript are available from the Dryad Digital Repository (<https://datadryad.org/10.5061/dryad.n02v6wx04>).

## ORCID

Songbo Tang  <https://orcid.org/0000-0001-9334-8089>

Jianfeng Liu  <https://orcid.org/0000-0002-5502-0872>

Frank S. Gilliam  <https://orcid.org/0000-0002-5525-0766>

Peter Hietz  <https://orcid.org/0000-0002-0458-6593>

Zhiheng Wang  <https://orcid.org/0000-0003-0808-7780>

Xiankai Lu  <https://orcid.org/0000-0001-7720-6048>

Enqing Hou  <https://orcid.org/0000-0003-4864-2347>

Yunting Fang  <https://orcid.org/0000-0001-7531-546X>

Zhiqun Huang  <https://orcid.org/0000-0002-8929-4863>

Dianxiang Zhang  <https://orcid.org/0000-0001-6549-8872>

Rong Wang  <https://orcid.org/0000-0003-1962-0165>

Yuanwen Kuang  <https://orcid.org/0000-0003-0627-9519>

## REFERENCES

- Allan, R., Pereira, L., & Smith, M. (1998). *Crop evapotranspiration-Guidelines for computing crop water requirements-FAO Irrigation and drainage paper 56* (Vol. 56). FAO-Food and Agriculture Organization of the United Nations.
- Amundson, R., Austin, A. T., Schuur, E. A. G., Yoo, K., Matzek, V., Kendall, C., Uebersax, A., Brenner, D., & Baisden, W. T. (2003). Global patterns of the isotopic composition of soil and plant nitrogen. *Global Biogeochemical Cycles*, 17(1), 1031. <https://doi.org/10.1029/2002GB001903>
- Asseng, S., Foster, I., & Turner, N. C. (2011). The impact of temperature variability on wheat yields. *Global Change Biology*, 17(2), 997–1012. <https://doi.org/10.1111/j.1365-2486.2010.02262.x>
- Azen, R., & Budesu, D. V. (2003). The dominance analysis approach for comparing predictors in multiple regression. *Psychological Methods*, 8(2), 129–148. <https://doi.org/10.1037/1082-989x.8.2.129>
- Bartoń, K. (2018). MuMIn: Multi-Model Inference (Version 1.40.4) [Computer software]. Retrieved from <https://CRAN.R-project.org/package=MuMIn>
- BassiriRad, H., Constable, J. V. H., Lussenhop, J., Kimball, B. A., Norby, R. J., Oechel, W. C., Reich, P. B., Schlesinger, W. H., Zitzer, S., Sehtiya, H. L., & Silim, S. (2003). Widespread foliage  $\delta^{15}\text{N}$  depletion under elevated  $\text{CO}_2$ : inferences for the nitrogen cycle. *Global Change Biology*, 9(11), 1582–1590. <https://doi.org/10.1046/j.1365-2486.2003.00679.x>
- Caldararu, S., Thum, T., Yu, L., Kern, M., Nair, R., & Zaehle, S. (2022). Long-term ecosystem nitrogen limitation from foliar  $\delta^{15}\text{N}$  data and a land surface model. *Global Change Biology*, 28(2), 493–508. <https://doi.org/10.1111/gcb.15933>
- Craine, J. M., Elmore, A. J., Aidar, M. P. M., Bustamante, M., Dawson, T. E., Hobbie, E. A., Kahmen, A., Mack, M. C., McLauchlan, K. K., Michelsen, A., Nardoto, G. B., Pardo, L. H., Peñuelas, J., Reich, P. B., Schuur, E. A. G., Stock, W. D., Templer, P. H., Virginia, R. A., Welker, J. M., ... Wright, I. J. (2009). Global patterns of foliar nitrogen isotopes and their relationships with climate, mycorrhizal fungi, foliar nutrient concentrations, and nitrogen availability. *New Phytologist*, 183(4), 980–992. <https://doi.org/10.1111/j.1469-8137.2009.02917.x>
- Craine, J. M., Elmore, A. J., Wang, L., Aranibar, J., Bauters, M., Boeckx, P., Crowley, B. E., Dawes, M. A., Delzon, S., Fajardo, A., Fang, Y., Fujiyoshi, L., Gray, A., Guerrieri, R., Gundale, M. J., Hawke, D. J., Hietz, P., Jonard, M., Kearsley, E., ... Zmudczyńska-Skarbek, K. (2018). Isotopic evidence for oligotrophication of terrestrial ecosystems. *Nature Ecology & Evolution*, 2(11), 1735–1744. <https://doi.org/10.1038/s41559-018-0694-0>
- Dai, Z., Yu, M., Chen, H., Zhao, H., Huang, Y., Su, W., Xia, F., Chang, S. X., Brookes, P. C., Dahlgren, R. A., & Xu, J. (2020). Elevated temperature shifts soil N cycling from microbial immobilization to enhanced mineralization, nitrification and denitrification across global terrestrial ecosystems. *Global Change Biology*, 26(9), 5267–5276. <https://doi.org/10.1111/gcb.15211>
- Elmore, A. J., Nelson, D. M., & Craine, J. M. (2016). Earlier springs are causing reduced nitrogen availability in North American eastern deciduous forests. *Nature Plants*, 2(10), 16133. <https://doi.org/10.1038/nplants.2016.133>
- Evans, R. D. (2001). Physiological mechanisms influencing plant nitrogen isotope composition. *Trends in Plant Science*, 6(3), 121–126. [https://doi.org/10.1016/s1360-1385\(01\)01889-1](https://doi.org/10.1016/s1360-1385(01)01889-1)
- Fang, Y., Yoh, M., Koba, K., Zhu, W., Takebayashi, Y., Xiao, Y., Lei, C., Mo, J., Zhang, W., & Lu, X. (2011). Nitrogen deposition and forest nitrogen cycling along an urban-rural transect in southern China. *Global Change Biology*, 17(2), 872–885. <https://doi.org/10.1111/j.1365-2486.2010.02283.x>
- Felix, J. D., & Elliott, E. M. (2014). Isotopic composition of passively collected nitrogen dioxide emissions: Vehicle, soil and livestock source signatures. *Atmospheric Environment*, 92, 359–366. <https://doi.org/10.1016/j.atmosenv.2014.04.005>
- Felix, J. D., Elliott, E. M., & Gay, D. A. (2017). Spatial and temporal patterns of nitrogen isotopic composition of ammonia at U.S. ammonia monitoring network sites. *Atmospheric Environment*, 150, 434–442. <https://doi.org/10.1016/j.atmosenv.2016.11.039>
- Fick, S. E., & Hijmans, R. J. (2017). WorldClim 2: new 1-km spatial resolution climate surfaces for global land areas. *International Journal of Climatology*, 37(12), 4302–4315. <https://doi.org/10.1002/joc.5086>
- Galloway, J. N., Townsend, A. R., Erisman, J. W., Bekunda, M., Cai, Z., Freney, J. R., Martinelli, L. A., Seitzinger, S. P., & Sutton, M. A. (2008). Transformation of the nitrogen cycle: Recent trends, questions, and potential solutions. *Science*, 320(5878), 889–892. <https://doi.org/10.1126/science.1136674>
- Garten, C. T. (1993). Variation in foliar  $^{15}\text{N}$  abundance and the availability of soil-nitrogen on walker branch watershed. *Ecology*, 74(7), 2098–2113. <https://doi.org/10.2307/1940855>
- Gilliam, F. S., Burns, D. A., Driscoll, C. T., Frey, S. D., Lovett, G. M., & Watmough, S. A. (2019). Decreased atmospheric nitrogen deposition in eastern North America: Predicted responses of forest ecosystems. *Environmental Pollution*, 244, 560–574. <https://doi.org/10.1016/j.envpol.2018.09.135>
- Gilliam, F. S., Walter, C. A., Adams, M. B., & Peterjohn, W. T. (2018). Nitrogen (N) dynamics in the mineral soil of a central appalachian hardwood forest during a quarter century of whole-watershed N additions. *Ecosystems*, 21(8), 1489–1504. <https://doi.org/10.1007/s10021-018-0234-4>
- Gong, X., Xu, Z., Peng, Q., Tian, Y., Hu, Y., Li, Z., & Hao, T. (2021). Spatial patterns of leaf  $\delta^{13}\text{C}$  and  $\delta^{15}\text{N}$  of aquatic macrophytes in the arid zone of northwestern China. *Ecology and Evolution*, 11(7), 3110–3119. <https://doi.org/10.1002/ece3.7257>
- Gremer, J. R., Andrews, C., Norris, J. R., Thomas, L. P., Munson, S. M., Duniway, M. C., & Bradford, J. B. (2018). Increasing temperature seasonality may overwhelm shifts in soil moisture to favor shrub over grass dominance in Colorado Plateau drylands. *Oecologia*, 188(4), 1195–1207. <https://doi.org/10.1007/s00442-018-4282-4>

- Grossiord, C., Buckley, T. N., Cernusak, L. A., Novick, K. A., Poulter, B., Siegwolf, R. T. W., Sperry, J. S., & McDowell, N. G. (2020). Plant responses to rising vapor pressure deficit. *New Phytologist*, 226(6), 1550–1566. <https://doi.org/10.1111/nph.16485>
- Harris, I., Jones, P. D., Osborn, T. J., & Lister, D. H. (2014). Updated high-resolution grids of monthly climatic observations - the CRU TS3.10 Dataset. *International Journal of Climatology*, 34(3), 623–642. <https://doi.org/10.1002/joc.3711>
- Hastings, M. G., Jarvis, J. C., & Steig, E. J. (2009). Anthropogenic impacts on nitrogen isotopes of ice-core nitrate. *Science*, 324(5932), 1288–1288. <https://doi.org/10.1126/science.1170510>
- Heaton, T. H. E. (1990).  $^{15}\text{N}/^{14}\text{N}$  ratios of  $\text{NO}_x$  from vehicle engines and coal-fired power stations. *Tellus B*, 42(3), 304–307. <https://doi.org/10.1034/j.1600-0889.1990.00007.x-1>
- Hietz, P., Duenisch, O., & Wanek, W. (2010). Long-term trends in nitrogen isotope composition and nitrogen concentration in Brazilian rainforest trees suggest changes in nitrogen cycle. *Environmental Science & Technology*, 44(4), 1191–1196. <https://doi.org/10.1021/es901383g>
- Hietz, P., Turner, B. L., Wanek, W., Richter, A., Nock, C. A., & Wright, S. J. (2011). Long-term change in the nitrogen cycle of tropical forests. *Science*, 334(6056), 664–666. <https://doi.org/10.1126/science.1211979>
- Hiltbrunner, E., Korner, C., Meier, R., Braun, S., & Kahmen, A. (2019). Data do not support large-scale oligotrophication of terrestrial ecosystems. *Nature Ecology & Evolution*, 3(9), 1285–1286. <https://doi.org/10.1038/s41559-019-0948-5>
- Höbber, E. A., & Höbber, P. (2012). Nitrogen isotopes link mycorrhizal fungi and plants to nitrogen dynamics. *New Phytologist*, 196(2), 367–382. <https://doi.org/10.1111/j.1469-8137.2012.04300.x>
- Högberg, P. (1997).  $^{15}\text{N}$  natural abundance in soil-plant systems. *New Phytologist*, 137(2), 179–203. <https://doi.org/10.1046/j.1469-8137.1997.00808.x>
- Houlton, B. Z., Sigman, D. M., & Hedin, L. O. (2006). Isotopic evidence for large gaseous nitrogen losses from tropical rainforests. *Proceedings of the National Academy of Sciences of the United States of America*, 103(23), 8745–8750. <https://doi.org/10.1073/pnas.0510185103>
- Krishna, M. P., & Mohan, M. (2017). Litter decomposition in forest ecosystems: A review. *Energy, Ecology and Environment*, 2(4), 236–249. <https://doi.org/10.1007/s40974-017-0064-9>
- Li, Z., Hastings, M. G., Walters, W. W., Tian, L., Clemens, S. C., Song, L., Shao, L., & Fang, Y. (2020). Isotopic evidence that recent agriculture overprints climate variability in nitrogen deposition to the Tibetan Plateau. *Environment International*, 138, 105614. <https://doi.org/10.1016/j.envint.2020.105614>
- Lihavainen, J., Ahonen, V., Keski-Saari, S., Kontunen-Soppela, S., Oksanen, E., & Keinanen, M. (2016). Low vapour pressure deficit affects nitrogen nutrition and foliar metabolites in silver birch. *Journal of Experimental Botany*, 67(14), 4353–4365. <https://doi.org/10.1093/jxb/erw218>
- Liu, X., Duan, L., Mo, J., Du, E., Shen, J., Lu, X., Zhang, Y., Zhou, X., He, C., & Zhang, F. (2011). Nitrogen deposition and its ecological impact in China: An overview. *Environmental Pollution*, 159(10), 2251–2264. <https://doi.org/10.1016/j.envpol.2010.08.002>
- Liu, X., Zhang, Y., Han, W., Tang, A., Shen, J., Cui, Z., Vitousek, P., Erisman, J. W., Goulding, K., Christie, P., Fangmeier, A., & Zhang, F. (2013). Enhanced nitrogen deposition over China. *Nature*, 494(7438), 459–462. <https://doi.org/10.1038/nature11917>
- Liu, X. Y., Xiao, H. Y., Liu, C. Q., Li, Y. Y., & Xiao, H. W. (2008). Tissue N content and  $^{15}\text{N}$  natural abundance in epilithic mosses for indicating atmospheric N deposition in the Guiyang area, SW China. *Applied Geochemistry*, 23(9), 2708–2715. <https://doi.org/10.1016/j.apgeochem.2008.06.002>
- Lu, C., & Tian, H. (2014). Half-century nitrogen deposition increase across China: A gridded time-series data set for regional environmental assessments. *Atmospheric Environment*, 97, 68–74. <https://doi.org/10.1016/j.atmosenv.2014.07.061>
- Lu, X., Mao, Q., Gilliam, F. S., Luo, Y., & Mo, J. (2014). Nitrogen deposition contributes to soil acidification in tropical ecosystems. *Global Change Biology*, 20(12), 3790–3801. <https://doi.org/10.1111/gcb.12665>
- Luo, Y., Hui, D. F., & Zhang, D. Q. (2006). Elevated  $\text{CO}_2$  stimulates net accumulations of carbon and nitrogen in land ecosystems: A meta-analysis. *Ecology*, 87(1), 53–63. <https://doi.org/10.1890/04-1724>
- Luo, Y., Su, B., Currie, W. S., Dukes, J. S., Finzi, A. C., Hartwig, U., Hungate, B., McMurtrie, R. E., Oren, R., Parton, W. J., Pataki, D. E., Shaw, M. R., Zak, D. R., & Field, C. B. (2004). Progressive nitrogen limitation of ecosystem responses to rising atmospheric carbon dioxide. *Bioscience*, 54(8), 731–739. [https://doi.org/10.1641/0006-3568\(2004\)054\[0731.pnloer\]2.0.co;2](https://doi.org/10.1641/0006-3568(2004)054[0731.pnloer]2.0.co;2)
- Marchand, W., Girardin, M. P., Hartmann, H., Depardieu, C., Isabel, N., Gauthier, S., Boucher, E., & Bergeron, Y. (2020). Strong overestimation of water-use efficiency responses to rising  $\text{CO}_2$  in tree-ring studies. *Global Change Biology*, 26, 4538–4558. <https://doi.org/10.1111/gcb.15166>
- Mason, R. E., Craine, J. M., Lany, N. K., Jonard, M., Ollinger, S. V., Groffman, P. M., Fulweiler, R. W., Angerer, J., Read, Q. D., Reich, P. B., Templer, P. H., & Elmore, A. J. (2022). Evidence, causes, and consequences of declining nitrogen availability in terrestrial ecosystems. *Science*, 376(6590), 261–272. <https://doi.org/10.1126/science.abh3767>
- McLauchlan, K. K., Craine, J. M., Oswald, W. W., Leavitt, P. R., & Likens, G. E. (2007). Changes in nitrogen cycling during the past century in a northern hardwood forest. *Proceedings of the National Academy of Sciences of the United States of America*, 104(18), 7466–7470. <https://doi.org/10.1073/pnas.0701779104>
- McLauchlan, K. K., Ferguson, C. J., Wilson, I. E., Ocheltree, T. W., & Craine, J. M. (2010). Thirteen decades of foliar isotopes indicate declining nitrogen availability in central North American grasslands. *New Phytologist*, 187(4), 1135–1145. <https://doi.org/10.1111/j.1469-8137.2010.03322.x>
- McLauchlan, K. K., Gerhart, L. M., Battles, J. J., Craine, J. M., Elmore, A. J., Higuera, P. E., Mack, M. C., McNeil, B. E., Nelson, D. M., Pederson, N., & Perakis, S. S. (2017). Centennial-scale reductions in nitrogen availability in temperate forests of the United States. *Scientific Reports*, 7, 7856. <https://doi.org/10.1038/s41598-017-08170-z>
- Pan, X., Baquy, M. A. A., Guan, P., Yan, J., Wang, R., Xu, R., & Xie, L. (2020). Effect of soil acidification on the growth and nitrogen use efficiency of maize in Ultisols. *Journal of Soils and Sediments*, 20(3), 1435–1445. <https://doi.org/10.1007/s11368-019-02515-z>
- Pardo, L. H., Semaoune, P., Schaberg, P. G., Eagar, C., & Sebilo, M. (2013). Patterns in  $\delta^{15}\text{N}$  in roots, stems, and leaves of sugar maple and American beech seedlings, saplings, and mature trees. *Biogeochemistry*, 112(1-3), 275–291. <https://doi.org/10.1007/s10533-012-9724-1>
- Pardo, L. H., Templer, P. H., Goodale, C. L., Duke, S., Groffman, P. M., Adams, M. B., Boeckx, P., Boggs, J., Campbell, J., Colman, B., Compton, J., Emmett, B., Gundersen, P., Kjonaas, J., Lovett, G., Mack, M., Magill, A., Mbila, M., Mitchell, M. J., ... Wessel, W. (2006). Regional assessment of N saturation using foliar and root  $\delta^{15}\text{N}$ . *Biogeochemistry*, 80(2), 143–171. <https://doi.org/10.1007/s10533-006-9015-9>
- Payne, R. J., Dise, N. B., Field, C. D., Dore, A. J., Caporn, S. J. M., & Stevens, C. J. (2017). Nitrogen deposition and plant biodiversity: past, present, and future. *Frontiers in Ecology and the Environment*, 15(8), 431–436. <https://doi.org/10.1002/fee.1528>
- Peng, S., Ding, Y., Liu, W., & Li, Z. (2019). 1 km monthly temperature and precipitation dataset for China from 1901 to 2017. *Earth System Science Data*, 11(4), 1931–1946. <https://doi.org/10.5194/essd-11-1931-2019>
- Peñuelas, J., & Estiarte, M. (1997). Trends in plant carbon concentration and plant demand for N throughout this century. *Oecologia*, 109(1), 69–73. <https://doi.org/10.1007/s004420050059>

- Peñuelas, J., & Filella, I. (2001). Herbaria century record of increasing eutrophication in Spanish terrestrial ecosystems. *Global Change Biology*, 7(4), 427–433. <https://doi.org/10.1046/j.1365-2486.2001.00421.x>
- Qu, L., Xiao, H., Guan, H., Zhang, Z., & Xu, Y. (2016). Total N content and  $\delta^{15}\text{N}$  signatures in moss tissue for indicating varying atmospheric nitrogen deposition in Guizhou Province, China. *Atmospheric Environment*, 142, 145–151. <https://doi.org/10.1016/j.atmosenv.2016.07.044>
- R Core Team. (2020). *R: A language and environment for statistical computing*. R Foundation for Statistical Computing. Retrieved from <https://www.R-project.org/>
- Rivero-Villar, A., Templer, P. H., Parra-Tabla, V., & Campo, J. (2018). Differences in nitrogen cycling between tropical dry forests with contrasting precipitation revealed by stable isotopes of nitrogen in plants and soils. *Biotropica*, 50(6), 859–867. <https://doi.org/10.1111/btp.12612>
- Salazar, K., & Mcnutt, M. K. (2012). Bioclimatic predictors for supporting ecological applications in the conterminous United States. In U.S. Geological Survey Data Series 691.
- Schimel, J. P., & Bennett, J. (2004). Nitrogen mineralization: Challenges of a changing paradigm. *Ecology*, 85(3), 591–602. <https://doi.org/10.1890/03-8002>
- Schmitz, A., Sanders, T. G. M., Bolte, A., Bussotti, F., Dirnboeck, T., Johnson, J., Penuelas, J., Pollastrini, M., Prescher, A.-K., Sardans, J., Verstraeten, A., & de Vries, W. (2019). Responses of forest ecosystems in Europe to decreasing nitrogen deposition. *Environmental Pollution*, 244, 980–994. <https://doi.org/10.1016/j.envpol.2018.09.101>
- Shan, Y., Huang, M., Suo, L., Zhao, X., & Wu, L. (2019). Composition and variation of soil  $\delta^{15}\text{N}$  stable isotope in natural ecosystems. *Catena*, 183, 104236. <https://doi.org/10.1016/j.catena.2019.104236>
- Tang, S., Lai, Y., Tang, X., Phillips, L. O., Liu, J., Chen, D., Wen, D., Wang, S., Chen, L., Tian, X., & Kuang, Y. (2021). Multiple environmental factors regulate the large-scale patterns of plant water use efficiency and nitrogen availability across China's forests. *Environmental Research Letters*, 16, 034026. <https://doi.org/10.1088/1748-9326/abe3bb>
- Townsend, A. R., Cleveland, C. C., Asner, G. P., & Bustamante, M. M. C. (2007). Controls over foliar N:P ratios in tropical rain forests. *Ecology*, 88(1), 107–118. [https://doi.org/10.1890/0012-9658\(2007\)88\[107:COFNRI\]2.0.CO;2](https://doi.org/10.1890/0012-9658(2007)88[107:COFNRI]2.0.CO;2)
- Vallano, D. M., & Sparks, J. P. (2013). Foliar  $\delta^{15}\text{N}$  is affected by foliar nitrogen uptake, soil nitrogen, and mycorrhizae along a nitrogen deposition gradient. *Oecologia*, 172(1), 47–58. <https://doi.org/10.1007/s00442-012-2489-3>
- van der Slepen, P., Vlam, M., Groenendijk, P., Anten, N. P. R., Bongers, F., Bunyavejchewin, S., Hietz, P., Pons, T. L., & Zuidema, P. A. (2015).  $^{15}\text{N}$  in tree rings as a bio-indicator of changing nitrogen cycling in tropical forests: an evaluation at three sites using two sampling methods. *Frontiers in Plant Science*, 6. <https://doi.org/10.3389/fpls.2015.00229>
- Vitousek, P. M., & Sanford, R. L. (1986). Nutrient cycling in moist tropical forest. *Annual Review of Ecology and Systematics*, 17, 137–167. <https://doi.org/10.1146/annurev.es.17.110186.001033>
- Wang, J., Feng, L., Palmer, P. I., Liu, Y., Fang, S., Bosch, H., O'Dell, C. W., Tang, X., Yang, D., Liu, L., & Xia, C. (2020). Large Chinese land carbon sink estimated from atmospheric carbon dioxide data. *Nature*, 586(7831), 720–723. <https://doi.org/10.1038/s41586-020-2849-9>
- Wang, R., Goll, D., Balkanski, Y., Hauglustaine, D., Boucher, O., Ciais, P., Janssens, I., Penuelas, J., Guenet, B., Sardans, J., Bopp, L., Vuichard, N., Zhou, F., Li, B. G., Piao, S. L., Peng, S. S., Huang, Y., & Tao, S. (2017). Global forest carbon uptake due to nitrogen and phosphorus deposition from 1850 to 2100. *Global Change Biology*, 23(11), 4854–4872. <https://doi.org/10.1111/gcb.13766>
- Wolf, K., Veldkamp, E., Homeier, J., & Martinson, G. O. (2011). Nitrogen availability links forest productivity, soil nitrous oxide and nitric oxide fluxes of a tropical montane forest in southern Ecuador. *Global Biogeochemical Cycles*, 25, GB4009. <https://doi.org/10.1029/2010gb003876>
- Yu, G., Jia, Y., He, N., Zhu, J., Chen, Z., Wang, Q., Piao, S., Liu, X., He, H., Guo, X., Wen, Z., Li, P., Ding, G., & Goulding, K. (2019). Stabilization of atmospheric nitrogen deposition in China over the past decade. *Nature Geoscience*, 12(6), 424–429. <https://doi.org/10.1038/s41561-019-0352-4>
- Yuan, W., Zheng, Y., Piao, S., Ciais, P., Lombardozzi, D., Wang, Y., Ryu, Y., Chen, G., Dong, W., Hu, Z., Jain, A. K., Jiang, C., Kato, E., Li, S., Lienert, S., Liu, S., Nabel, J. E. M. S., Qin, Z., Quine, T., ... Yang, S. (2019). Increased atmospheric vapor pressure deficit reduces global vegetation growth. *Science Advances*, 5(8), eaax1396. <https://doi.org/10.1126/sciadv.aax1396>
- Zhao, J., Zhang, Z., Zhu, G., Zheng, N., Xiao, H., Tian, J., Zhou, Y., Guan, H., & Xiao, H. (2019). The  $\delta^{15}\text{N}$  values of epilithic mosses indicating the changes of nitrogen sources in Guiyang (SW China) from 2006 to 2016–2017. *Science of the Total Environment*, 696, 133988. <https://doi.org/10.1016/j.scitotenv.2019.133988>
- Zhao, X., Liu, S. L., Pu, C., Zhang, X. Q., Xue, J. F., Zhang, R., Wang, Y. Q., Lal, R., Zhang, H. L., & Chen, F. (2016). Methane and nitrous oxide emissions under no-till farming in China: A meta-analysis. *Global Change Biology*, 22(4), 1372–1384. <https://doi.org/10.1111/gcb.13185>
- Zhao, Y., Xi, M., Zhang, Q., Dong, Z., Ma, M., Zhou, K., Xu, W., Xing, J., Zheng, B., Wen, Z., Liu, X., Nielsen, C. P., Liu, Y., Pan, Y., & Zhang, L. (2022). Decline in bulk deposition of air pollutants in China lags behind reductions in emissions. *Nature Geoscience*, 15, 190–195. <https://doi.org/10.1038/s41561-022-00899-1>
- Zhou, G., Houlton, B. Z., Wang, W., Huang, W., Xiao, Y., Zhang, Q., Liu, S., Cao, M., Wang, X., Wang, S., Zhang, Y., Yan, J., Liu, J., Tang, X., & Zhang, D. (2014). Substantial reorganization of China's tropical and subtropical forests: based on the permanent plots. *Global Change Biology*, 20(1), 240–250. <https://doi.org/10.1111/gcb.12385>

## SUPPORTING INFORMATION

Additional supporting information may be found in the online version of the article at the publisher's website.

**How to cite this article:** Tang, S., Liu, J., Gilliam, F. S., Hietz, P., Wang, Z., Lu, X., Zeng, F., Wen, D., Hou, E., Lai, Y., Fang, Y., Tu, Y., Xi, D., Huang, Z., Zhang, D., Wang, R., & Kuang, Y. (2022). Drivers of foliar  $^{15}\text{N}$  trends in southern China over the last century. *Global Change Biology*, 28, 5441–5452. <https://doi.org/10.1111/gcb.16285>